IJCMBS

THE INTERNATIONAL JOURNAL OF CURRENT MEDICAL AND BIOLOGICAL SCIENCES e-ISSN: 2791-8815

Orgınal Article

Histopathological Evaluation of The Protective Effects of Resveratrol Against Gastrointestinal Tissue Damage Induced by Cisplatin in Rats

Sıçanlarda Sisplatin Tarafından İndüklenen Gastrointestinal Doku Hasarına Karşı Resveratrolün Koruyucu Etkilerinin Histolopatolojik Olarak Değerlendirilmesi

Hatice Hancı[1*], Sibel Türedi2

[1]Department of Histology and Embryology, Ordu University, Faculty of Medicine, Ordu,Türkiye
[2]Department of Histology and Embryology, Harran University, Faculty of Medicine, Türkiye

**Corresponding author:*
Hatice Hancı
Adress: 1Department of Histology and Embryology, Ordu University, Faculty of Medicine, Ordu,Türkiye
E-mail: haticehancii@gmail.com

Received: 23/05/2023
Accepted: 17/06/2023
Cite as: HANCI. H and TUREDİ.S. Histopathological Evaluation of The Protective Effects of Resveratrol Against Gastrointestinal Tissue Damage Induced by Cisplatin in Rats IJCMBS 2023;3(2):95-104
doi.org/ 10.5281/zenodo.8050827

Highlights

- Cisplatin renders the metabolically active intestinal mucosa highly susceptible to cytotoxic effects.
- The resveratrol application demonstrates a dose-dependent protective effect against intestinal damage caused by cisplatin.

Abstract

Background: The purpose of this study was to investigate the effects of differing doses of resveratrol (RES) against cisplatin (CP)-induced gastrointestinal injury in small intestinal tissue using histopathological and immunohistochemical methods.
Materials and Methods: Forty-eight healthy male Wistar albino rats aged 12-16 weeks were divided into eight groups, control RES-30, RES-60, RES-90, CP, CP+RES30, CP+RES60, and CP+RES90. Small intestine tissues were collected at the end of the experimental period and subjected to routine Hematoxylin & Eosin (H&E) and Periodic Acid Schiff (PAS) staining. Tumor necrosis factor alpha (TNF-α) and interleukin 1 beta (IL-1β) were evaluated from immunohistochemically stained tissues. DNA fragmentation was evaluated using the TUNEL technique.
Results: Based on the histopathological findings, vacuolization and shedding were observed in the small intestine surface epithelium with notable fusion and shortening in the villus structure in the CP group. Significant decreases were observed in the CP+RES30, CP+RES60, and particularly CP+RES90 groups compared to the CP group in terms of apical surface epithelial degeneration, villous fusion, and inflammatory cell infiltration. The apoptotic index (AI) and TNF-α immunoreactivities were significantly higher in the CP group ($p<0.05$). AI and TNF-α immune intensity were significantly lower in the treatment groups ($p<0.05$). It has been determined that among the treatment groups, particularly the CP+RES30 group showed the lowest damage score values and immunoreactivity of TNF-α with AI.**Conclusions:** CP caused severe histological tissue injury, intestinal apoptosis, and proinflammatory cytokine release, while RES administered before CP treatment exhibited a dose-dependent protective effect (particularly at RES30 mg/kg) against CP-induced intestinal injury.

Key Words: Cisplatin, Resveratrol, Histopathology, Small Intestine, Apoptosis

ÖZ Amaç: Çalışmamızda, Resveratrolün (RES) farklı dozlarının sıçanlarda Sisplatinin (CP) indüklediği gastrointestinal hasara karşı olan etkisini ince bağırsak dokusunda histopatolojik ve immunohistokimyasal yöntemler ile araştırmayı amaçladık. **Gereç ve yöntem:** Çalışmada, 12-16 haftalık sağlıklı 48 adet Wistar Albino cinsi erişkin erkek sıçanlar kullanıldı ve kontrol, RES-30, RES-60, RES-90, CP, CP+RES30, CP+RES60 ve CP+RES90 olmak üzere 8 gruba ayrıldı. Deneysel sürenin sonunda ince bağırsak dokuları Hematoksilen & Eosin (H&E) ile Periyodik Asit Schiff (PAS) boyamasına tabi tutuldu. Tümör nekroz faktörü alfa (TNF-α) ve interlökin 1 beta (IL-1β) immünhistokimyasal olarak boyanmış dokularda, DNA fragmentasyonu ise TUNEL tekniği kullanılarak değerlendirildi.n**Bulgular:** Çalışma bulgularına göre CP grubunun incelenmesinde, ince bağırsak yüzey epitelyumunda ciddi oranda vakualizasyon ve dökülme ile birlikte villus yapılarında kısalma ve füzyon dikkati çekmiştir. Tedavi gruplarının değerlendirilmesinde ise, CP grubuna kıyasla sırası ile CP+RES30, CP+RES60 ve CP+RES90 gruplarında apikal yüzey epitelyal dejenerasyonunun, villar füzyon oluşumunun ve inflamatuar hücre infiltrasyonunun anlamlı ölçüde azaldığı görülmüştür. Apoptotik indeks (AI) ile TNF-α immünreaktiflikleri, CP grubuna kıyasla kontrol grubunda önemli ölçüde yüksekti ($p<0,05$). AI ve TNF-α immün yoğunluğu, CP+RES30, CP+RES60 ve CP+RES90 gruplarında, CP grubuna kıyasla önemli ölçüde daha düşüktü ($p<0,05$). Tedavi grupları arasında özellikle CP+RES30 grubunun hasar skoru değerlerinin ve AI ile TNF-α immünreaktifliklerinin CP grubuna kıyasla en aza indiği belirlenmiştir.**Sonuç:** CP'nin şiddetli histolojik doku hasarına, bağırsak apoptozuna ve proinflamatuar sitokin salınımına neden olduğu, ancak CP tedavisinden önce uygulanan RES'in, CP'nin neden olduğu bağırsak hasarına karşı doza bağımlı (özellikle RES30 mg/kg) koruyucu etki gösterdiği belirlenmiştir.

Anahtar Kelimeler: Sisplatin, Resveratrol, Histopatoloji, İnce bağırsak, Apoptozis

Introduction

Cisplatin (MF-Cl2H6N2Pt, CP) cis-diamminedichloroplatinum II is one of the most potent DNA-modifying chemotherapeutic agents and plays an important role in the treatment of human solid tumors. CP cytotoxicity is associated with its capacity to cause inter- and intrastrand cross-linking, to interfere with the DNA repair mechanism, to cause DNA damage, to inhibit DNA replication mechanisms and/or transcription, and thus to induce apoptosis in cancer cells (1).

CP remains the main antiproliferative drug among the various therapeutic protocols, and is widely employed, with cure rates exceeding 90%, in the treatment of cancers of the bladder, head and neck, esophagus, testis, and ovaries, and in small cell lung cancers (2). Despite its many side-effects, including renal dysfunction, hepatotoxicity, neurotoxicity, myelosuppression, spermiotoxicity, and ototoxicity (3), CP is also the principal drug used in the therapeutic protocol for advanced gastrointestinal cancers (4). In terms of CP's known toxicity profile, the principal dose-limiting side-effect is nephrotoxicity. However, gastrointestinal symptoms present as a lifelong dominant clinical problem (1). The rapidly proliferating cells of the gastrointestinal epithelium mean that the gut is particularly vulnerable to the cytotoxic effects of CP. Chemotherapeutic agents, including CP, are capable of inducing wide morphological alterations (such as delayed gastric motility, diarrhea, and mucositis) that have a significant impact on adherence to treatment (3).

Extracts obtained from plant materials have historically been employed in the treatment of various diseases. RES is an endogenous agent found in various foodstuffs including grape, blueberry, and peanut. Chemically, it is known as trans-3,4,5-trihydroxystilbene, or more commonly as RES. It is a member of the stilbene family (synthetic aromatic hydrocarbon) and possesses geometric stereoisomers in cis and trans conformations (5). Research into the biological activities of RES has increased in recent years and has emphasized its antioxidant, anti-inflammatory, antiapoptotic, antiplatelet, antiatherogenic, and anticancer properties. RES is a polyphenolic phytoalexin present in grape, red wine, chocolate, Japanese knotweed root, peanut, mulberry, carnelian cherry, and Vaccinium plants such as blueberry (7).

Due to the risks associated with traditional cancer treatment methods, the use of this compound is particularly important in cancer patients (8). However, only a limited number of publications have examined the effect of RES in reducing the tumor burden in such patients. Moreover, no studies have investigated the dose-dependent effect of RES on CP-related gastrointestinal toxicity. Since CP is also absorbed by passive diffusion throughout the gastrointestinal system, the purpose of this study was to investigate the effects of differing doses of RES against CP-induce gastrointestinal damage in rats using histopathological, histomorphometric, and immunohistochemical methods.

Material and Method

Experimental Study Plan

This experimental study commenced following receipt of approval from the Harran University animal experiments local ethical committee (HAYDEK) (study protocol license no. 2022/006/20). The male Wistar albino rats used in the research were obtained from the Harran University Surgical Application and Research Center. Throughout the experiment, all rats were housed at a room temperature of 22 ± 2◦C, in 50% ± 10 humidity, and in a 12-h light:dark cycle. All rats were allowed ad libitum access to standard rat chow and tap water. All animals received humane care in line with the criteria outlined in the ‘‘Guide for the Care and Use of Laboratory Animals’’ published by the National Institutes of Health.

Establishment of the Experimental Animal Groups

The number of animals to be employed in the study was determined on the basis of the 3R3 principle and in consideration of avoidance of unnecessary animal use. Forty-eight healthy male Wistar albino rats aged 12-16 weeks and weighing 350-400 g were divided into eight groups. Control group, (C; n=6); Not subjected to any procedure. Resveratrol 30 mg group, (RES-30; n=6); RES 30 mg/kg per day (9) was dissolved in dimethyl sulfoxide (DMSO) and administered by the intragastric route for eight days. Resveratrol 60 mg group, (RES-60; n=6); RES 60 mg/kg per day administered by the intragastric route for eight days. Resveratrol 90 mg group, (RES-90; n=6); RES 90 mg/kg per day administered by the intragastric route for eight days. Cisplatin group, (CP; n=6); No procedure was performed for the first five of the eight day experimental period days. On the fifth day, a single dose of CP 16 mg/kg (10) was administered via the intraperitoneal (i.p.) route. Cisplatin+Resveratrol 30 mg group, (CP+RES30; n=6); RES 30 mg/kg per day was administered via the intragastric route for five days. On the fifth day, a single dose of CP 16 mg/kg was administered i.p., and RES 30 mg/kg per day was administered via the intragastric route for the following three days.

Cisplatin+Resveratrol 60 mg group, (CP+RES60; n=6); RES 60 mg/kg per day was administered via the intragastric route for five days. On the fifth day, a single dose of CP 16 mg/kg was administered i.p., and RES 60 mg/kg per day was administered via the intragastric route for the following three days. Cisplatin+Resveratrol 90 mg group, (CP+RES90; n=6); RES 90 mg/kg per day was administered via the intragastric route for five days. On the fifth day, a single dose of CP 16 mg/kg was administered i.p., and RES 90 mg/kg per day was administered via the intragastric route for the following three days.

Histological Methods

Tissue Preparation Procedures for Morphometric Measurements

At the end of the experimental period (day 8), all rats were sacrificed by exsanguination under deep anesthesia. A midline incision was first made, after which the small intestine was carefully and quickly severed and removed. Feces within the tissues were removed, and the specimens were fixed in 10% formalin solution. Following fixation, tissues collected for histological examinations were passed through 70%, 90%, 96%, and 100% alcohol series. After being rendered transparent with xylene, the tissues were embedded in paraffin blocks. Next, sections 5 µm in thickness were taken from the paraffin blocks using a fully automated microtome (Histo-Line ARM 3700, Pantigliate MI, Italy) and placed onto slides, before being stained with hematoxylin eosin (H&E) and PAS in order to reveal the general morphological characteristics of the small intestine tissues. All the histological layers of each tissue were subjected to separate histological examination under a light microscope at X40, X100, X200, and X400 magnifications. General gastrointestinal damage was scored semi-quantitatively based on specific criteria of apical surface epithelial degeneration, villar fusion, hemorrhage, and inflammatory cell infiltration (0: none; 1: mild; 2: moderate, and 3: severe), and a mean histopathological score was calculated for each experimental group (11). All tissue analyses were performed under a light microscope (Olympus BX 51; Olympus Optical Co. Ltd., Tokyo, Japan) on cellSens imaging software (Olympus Life Science Solution, Germany).

Immunohistochemical Methods

The Terminal Deoxynucleotidyl Transferase Biotin-dUTP Nick End Labeling (TUNEL) technique was used to evaluate apoptosis in the intestinal tissue. Cells exhibiting DNA fragmentation were identified using this technique. Cells with homogeneous staining and no necrotic areas, showing brown-stained nuclei and TUNEL positivity, were defined as apoptotic cells. The In Situ Cell Death Detection Kit (Roche, Mannheim, Germany) was used following the manufacturer's protocol for the TUNEL technique. The stained sections were examined under a light microscope (Olympus BX 51; Olympus Optical Co. Ltd., Tokyo, Japan) at 400X magnification, and a total of 100 cells were counted in 5 different areas to calculate the apoptotic index (AI) (AI = number of TUNEL-positive cells / total number of cells x 100) (12).

Paraffin-embedded blocks were sectioned into 5 µm thickness and then deparaffinized. Following that, the sections were washed with a PBS buffer solution for 5 minutes. Subsequently, the sections underwent antigen retrieval by boiling in citrate buffer at a pH of 6.0. To block endogenous peroxidase activity, the sections washed in PBS were treated with a 3% H_2O_2 solution. The specimens were then incubated with TNF-α (Santa Cruz Biotechnology Inc., cat no. sc-52746) and IL-1β (Santa Cruz Biotechnology Inc., cat no. sc-52012) antibodies, diluted to a 1:100 ratio, at a temperature of +4°C. The subsequent steps were carried out using secondary antibody kits (Thermo Scientific, MA, USA, cat no. TP-060-HL) following the manufacturer's instructions. For visualization, a 3,3'-Diaminobenzidine (DAB) chromogen kit was utilized (Sigma-Aldrich St. Louis, USA, cat no. D3939). The specimens were counterstained with Mayer's hematoxylin, covered and observed under a light microscope. Microphotographs were captured. For immunohistochemical analyses, three random areas were selected in each section. TNF-α and IL-1β positivity were identified by the presence of a brown color, and numerical evaluations were conducted. Scores were assigned based on the percentage frequency of TNF-α and IL-1β expression in the examined area: no expression (0), mild (1), moderate (2), strong (3), and very strong (4) expression. The percentage of positive cells was scored as follows: <5% positive expression (0), 6%-15% (1), 16%-50% (2), 51%-80% (3), and >80% (4) (13).

Statistical Analysis

All statistical analyses were performed using the SPSS 26.0 V software (Statistical Package for the Social Sciences, version 26.0, SSPS Inc., Chicago, IL, USA). All data were presented as standard deviation (SD) (±) mean. Kruskal Wallis analysis of variance was used to compare differences between group parameters. Dual comparisons between groups exhibiting significant values were evaluated with a Mann–Whitney U-test- with corrected Bonferroni test. Statistical significance was accepted for all tests at $p<0.05$.

Results

Histopathological Findings

All histopathological examinations of small intestinal tissues were conducted using sections stained with H&E and PAS. Examinations performed under light microscopy revealed preservation of the integrity of the lamina propria and epithelium in the small intestinal tissue mucosal layer, a normal histological structure in the brush border, enterocytes, and goblet cells, and preserved crypt/villus organization in tissues from the C, RES-30, and RES-60 groups. However, apical surface epithelium degeneration and fusion in villus structures were observed in the RES-90 compared to the control group **(Figure 1,2).**

CP group tissues exhibited severe vacuolization and shedding in the small intestine surface epithelium, together with shortening and fusion in villus structures. In addition to degeneration, the epithelium and lamina propria could not be distinguished, the villi lost their finger-like structure, and microvillus structures were impaired. Moreover, goblet cells lost their oval nucleus structure, and widespread inflammatory cell infiltration was observed in the mucosa, together with intense cystic formations **(Figure 1,2).** In terms of parameter analyses, gastrointestinal damage scores were significantly higher in the CP group than in the control group ($p<0.05$) **(Table, 1).**

Evaluation of the treatment groups showed significant decreases in apical surface epithelial degeneration, villous fusion, and inflammatory cell infiltration in the CP+RES30, CP+RES60, and CP+RES90 groups compared to the CP group ($p<0.05$) **(Table, 1).** Degeneration in epithelial cells and microvilli decreased, while villous structures were preserved. Although the treatment groups' histological findings were similar to one another, the damage score in the CP+RES30 group in particular decreased significantly compared to the CP group ($p<0.05$) **(Table 1).**

Table 1. The histological damage scores on the basis of analysis parameters and Immunohistochemical scores of the experimental groups

	Parameters						
	AI	**TNF-α**	**IL-1β**	**DASE**	**VF**	**ICI**	**H**
C	4.570±1.027	0.333±0.516	0.167±0.408	0.500±0.548	0.167±0.408	0.167±0.408	0.000 ± 0.000
RES30	5.342±1.194	0.500±0.548	0.333±0.516	0.667±0.516	0.333±0.516	0.333±0.516	0.000 ± 0.000
RES60	6.123±1.006[a]	0.667±0.816	0.167±0.408	0.833±0.753	0.833±0.408[a]	0.500±0.548	0.167 ± 0.408
RES90	8.232±0.852[a]	0.833±0.408	0.500±0.548	1.167±0.408[a]	1.333±0.516[a]	0.667±0.516	0.333 ± 0.516
CP	58.250±10.153[a]	2.500±0.548[a]	1.167±0.408[a]	2.667±0.516[a]	2.833±0.408[a]	1.667±0.516[a]	0.500 ± 0.548
CP+RES30	26.442±3.700[a,b]	0.833±0.408[b]	0.500±0.837	1.333±0.516[a,b]	1.167±0.408[a,b]	0.667±0.516[b]	0.167±0.408
CP+RES60	32.263±4.897[a,b]	1.000±0.632[a,b]	0.500±0.548	1.667±0.516[a,b]	1.500±0.548[a,b]	0.833±0.408[a,b]	0.333±0.516
CP+RES90	38.130±5.239[a,b,c]	1.500±0.548[a,b,c]	0.667±0.516	1.833±0.408[a,b]	1.667±0.516[a,b]	0.833±0.408[a,b]	0.333±0.516

Abberivations: The data represent means ± standard deviation; n = 6 for each group. RES; Resveratrol, CP; Cisplatin, AI; Apoptotic Index, TNF-α; Tumor Necrosis Factor-alpha, IL-1β; Interleukin-1 beta, DASE; Degeneration of the apical surface epithelium, VF; villar fusion, H; hemorrhage, ICI; inflammatory cell infiltration.**[a]; C** group values compared to all groups, ($p<0,05$).**[b]; CP** group values compared to the treatment groups (CP+RES30, CP+RES60, and CP+RES90), ($p<0,05$)**[c]; CP+RES30** group values compared to the CP+RES60 and CP+RES90 groups, ($p<0,05$).

Immunohistochemical Findings

Based on findings evaluated using the TUNEL technique, AI values in the CP group were significantly higher than those in the control group ($p<0.05$). AI values decreased in the CP+RES30, CP+RES60, and CP+RES90 groups compared with the CP group ($p<0.05$). No significant difference was observed between the AI values in the CP+RES30 and CP+RES60 groups ($p>0.05$), but AI values in the CP+RES90 group were significantly higher than those in the CP+RES30 group ($p<0.05$) **(Table 1, Figure 3).**

Analysis of TNF-α and IL-1β scores used to determine proinflammatory cytokine levels showed that TNF-α values in the CP group were significantly higher than those in the control group ($p<0.05$). In terms of the treatment groups, TNF-α values in the CP+RES30, CP+RES60, and CP+RES90 groups were significantly lower than those in the CP group g ($p<0.05$). While no significant difference was observed in TNF-α values between the CP+RES30 and CP+RES60 groups ($p>0.05$), they were significantly higher in the CP+RES90 group compared to the CP+RES30 group ($p<0.05$) **(Table 1**, **Figure 4).** No significant difference in IL-1β score findings was determined between the groups ($p>0.05$) **(Table 1, Figure 5).**

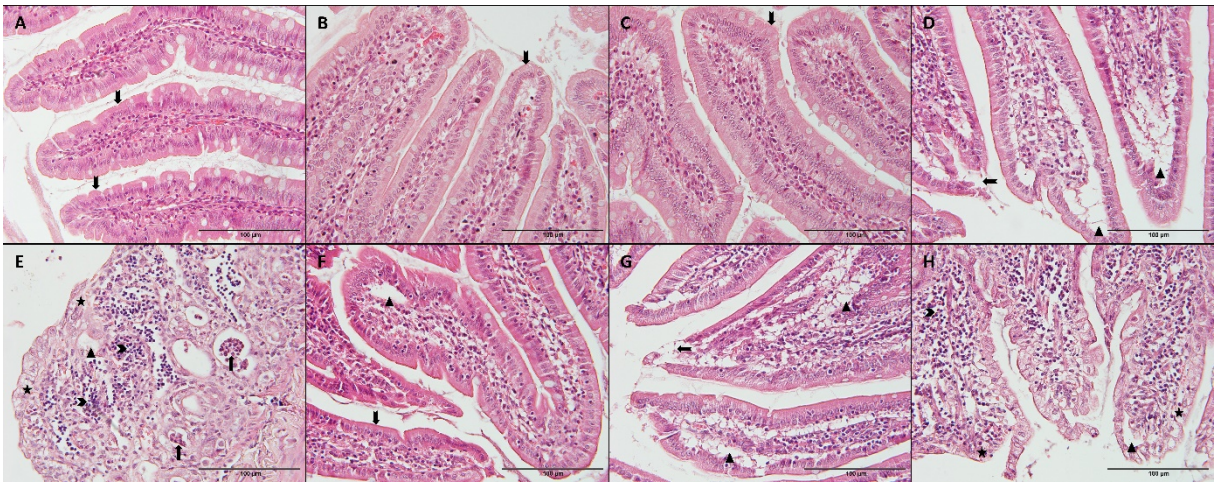

Figure 1. Light microscopic micrographs of rat small intestine sections stained with hematoxylin and eosin from control group (A), RES-30 **(B**), RES-60 **(C),** RES-90 **(D),** CP **(E),** CP+RES30 **(F),** CP+RES60 **(G),** and CP+RES90 **(H).** Normal villus structure with surface enterocytes and goblet cells (down notched arrow), vacuolization (triangle), shedding of surface enterocytes (left notched arrow), villar fusion accompanied by epithelial degeneration (asteriks), inflammatory cell infiltration (chevrons), cystic structures (up arrow), RES; Resveratrol, CP; Cisplatin, (Hematoxylin and eosin staining, X400).

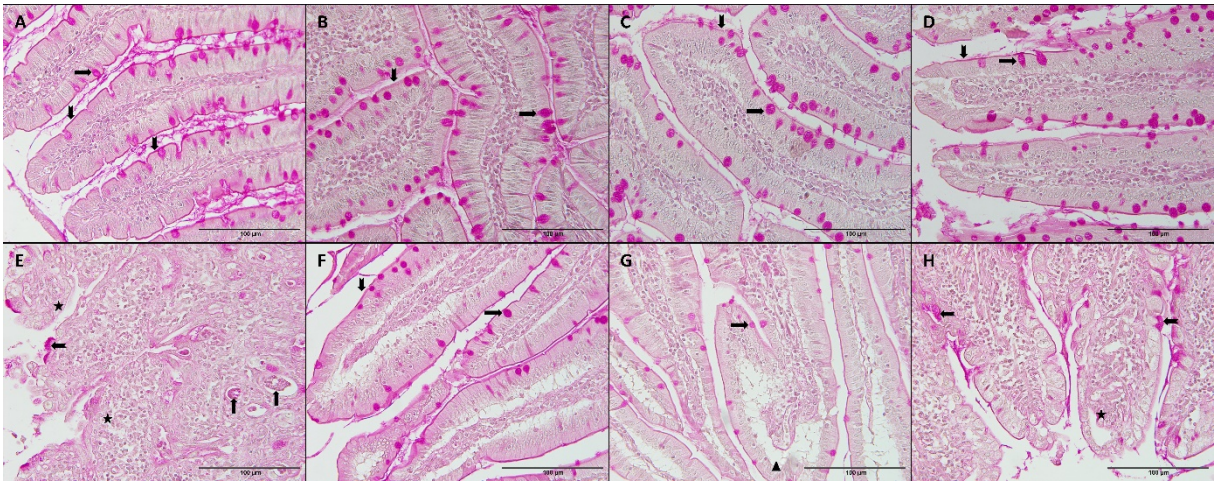

Figure 2. Light microscopic micrographs of rat small intestine sections stained with PAS from control group (A), RES-30 **(B)**, RES-60 **(C)**, RES-90 **(D)**, CP **(E)**, CP+RES30 **(F)**, CP+RES60 **(G)**, and CP+RES90 **(H)**. Normal villus structure with surface enterocytes (down notched arrow), normal goblet cells (right arrow), goblet cells lost their oval nucleus structure (left notched arrow), vacuolization (triangle), villar fusion accompanied by epithelial degeneration (asteriks), RES; Resveratrol, CP; Cisplatin, PAS; Periodic Acid Schiff, (PAS staining, X400).

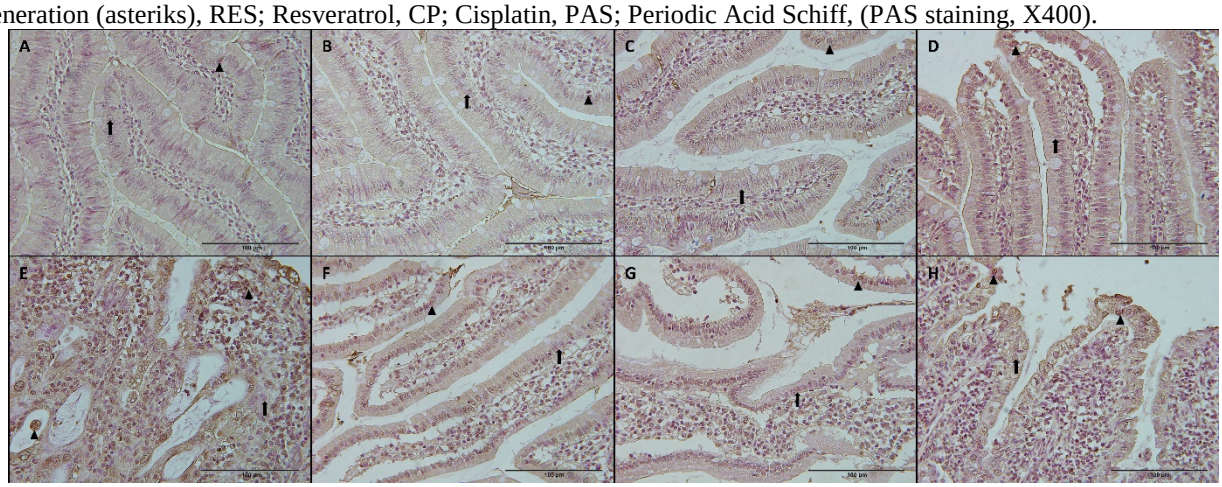

Figure 3. TUNEL-stained rat small intestine micrographs from control group (A), RES-30 **(B)**, RES-60 **(C)**, RES-90 **(D)**, CP **(E)**, CP+RES30 **(F)**, CP+RES60 **(G)**, and CP+RES90 **(H)**. Normal (up arrow) and TUNEL (+) (triangle) nucleus, RES; Resveratrol, CP; Cisplatin, TUNEL; The Terminal Deoxynucleotidyl Transferase Biotin-dUTP Nick End Labeling, (TUNEL, X400).

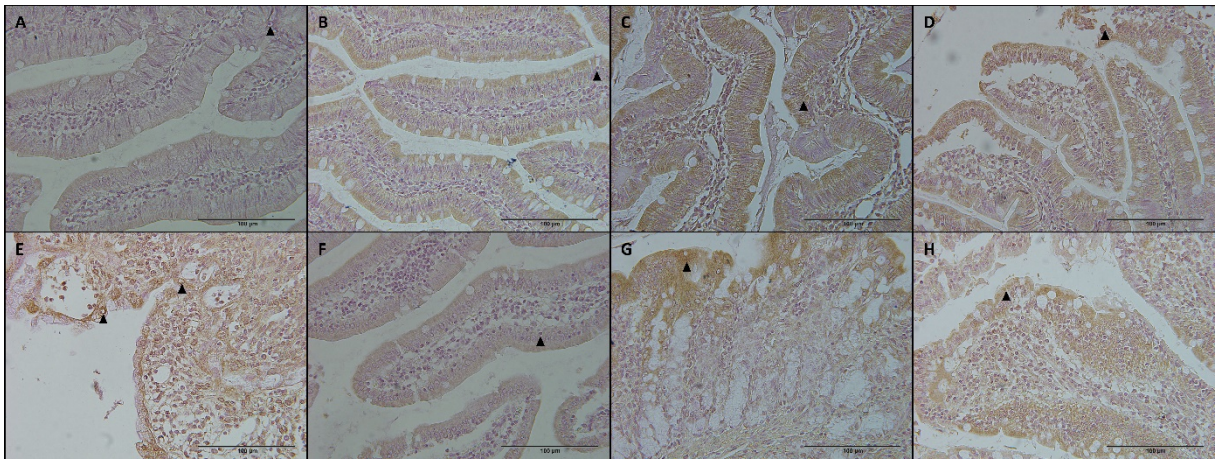

Figure 4. TNF-α-stained rat small intestine micrographs from control group (A), RES-30 **(B)**, RES-60 **(C)**, RES-90 **(D)**, CP **(E)**, CP+RES30 **(F)**, CP+RES60 **(G)**, and CP+RES90 **(H)**. TNF-α (+) cell (triangle), RES; Resveratrol, CP; Cisplatin, TNF-α; Tumor Necrosis Factor-alpha, (TNF-α, X400).

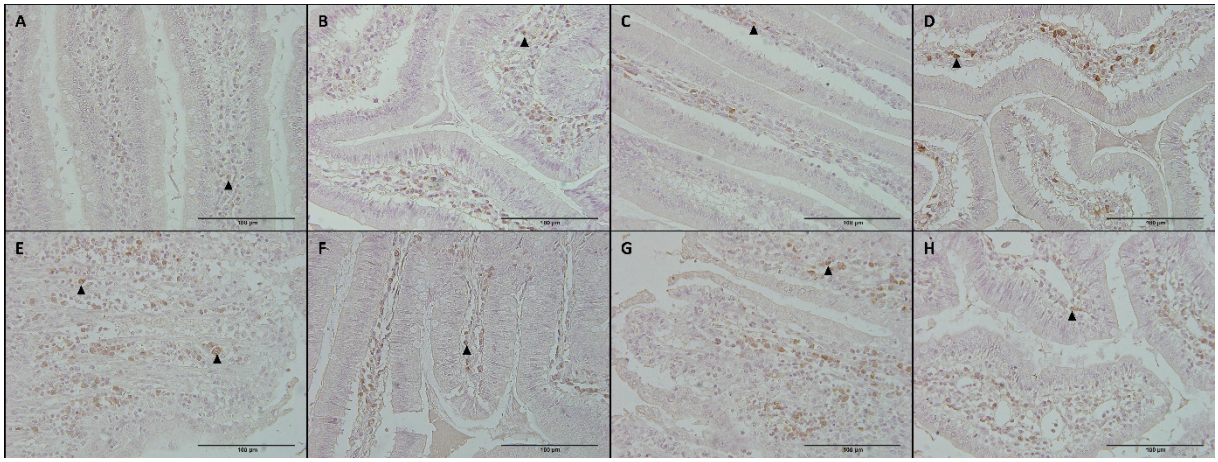

Figure 5. IL-1β-stained rat small intestine micrographs from control group (A), RES-30 **(B)**, RES-60 **(C)**, RES-90 **(D)**, CP **(E)**, CP+RES30 **(F)**, CP+RES60 **(G)**, and CP+RES90 **(H)**. IL-1β (+) cell (triangle), RES; Resveratrol, CP; Cisplatin, IL-1β; Interleukin-1 beta, (IL-1β, X400).

Discussion

CP, one of the most effective DNA-modifying chemotherapeutic agents, is a heavy metal complex exhibiting synergistic effects with various antitumor drugs and with no cross-resistance (14). However, in addition to its therapeutic benefits, CP and its metabolites can cause side-effects including nephrotoxicity, hepatotoxicity, and long-term gastrointestinal damage as a result of severe damage to the intestinal mucosa (15). Almost all patients can experience marked gastrointestinal side-effects due to CP-related intestinal dysfunction, generally consisting of varying degrees of nausea, diarrhea, mucositis, and delayed gastric motility (16,17). Although the clinical limitations of CP due to the side-effects described above have encouraged researchers to produce several CP analogues, the majority of platinum compounds exhibited no significant advantage over CP. For that reason, CP continues to be employed as a first-line drug in the treatment of several types of cancer, including those of the testis, prostate, ovary, cervix, bladder, and lung (16,18).

Due to its anatomical position, physiological characteristics, wide surface area, and high cell cycle, the small intestine is particularly susceptible to the adverse effects of chemotherapeutic agents such as CP. In addition, similarly to the majority of antineoplastic agents, CP is not target-specific, meaning that it affects all

proliferating cells and cause side-effects generally observed during cancer treatment (19). The brush border membrane, which covers the epithelial cells of the small intestine and performs various digestive and transport tasks, constitutes a highly differentiated cell membrane. The structural integrity of the intestinal mucosa, which is organized into crypts and villi in order to increase nutrient absorption and surface area, relies on the crypt cell production rate and the crypt/villus ratio. The gastrointestinal toxicity caused by CP is characterized by villus degeneration and desquamation, decreased villus height and density, crypt loss in structural terms, apoptosis and necrosis in intestinal epithelial cells, and glandular dilatation (20).

CP has the potential to stimulate widespread morphological variations in the intestinal mucosa. Studies showing that CP therapy lowers the total surface area of villi and microvilli, thus reducing intestinal motility, and causes changes in the intestine's digestive and metabolic functions have appeared in the literature. CP applied at low doses has been shown to cause villous atrophy but not to affect the crypt depth, thus reducing the villus/crypt ratio by approximately half. However, reports in the literature concerning high doses have shown that CP causes mucosal glandular distortion, inflammatory cell infiltration into the mucosal and submucosal layers, crypt ablation and abscess formation, villous degeneration, and decreased villous height (21,22). Zhang et al. (2022) also reported that CP injection caused a series of pathological changes leading to atrophy of the small intestine villi, crypt cell necrosis, epithelial cell shedding, and impairment of the submucosa and muscular layer (23).

In the present study of CP-induced gastrointestinal damage, and in agreement with previous research in the literature, severe vacuolization and shedding were observed in the small intestinal surface epithelium together with fusion and shortening in villous structures in the CP group. In addition to degeneration, the epithelium and lamina propria could not be distinguished in the mucosal layer, the villi lost their finger-like structure, and the structures of the microvilli were compromised. The goblet cells also lost their oval nucleus structures, and widespread inflammatory cell infiltration in the mucosa and intense cystic structures were detected. In a study investigating CP-related intestinal toxicity, Jin et al. (2022) reported breaks in villous structures as well as increased erythrocytes and inflammatory cells, decreased goblet cells, and degeneration in their CP group (24). Consistent with the literature, Yilmaz et al. (2022) also reported vacuolization in duodenal sections in the CP group, in addition to widespread necrotic epithelial cells, loss of microvillus structures, mucosal ulceration due to epithelial cell loss, and widespread inflammation in the lamina propria (25).

Patients being treated for cancer undergo a number of different therapeutic regimens, including the administration of cancer chemotherapy drugs, radiation, surgery, and immunotherapy. Treatment using chemotherapy agents is associated with a very high side-effect rate, ranging from milder effects such as nausea, vomiting, hair loss, and bone marrow suppression, to more serious manifestations including neuropathy, liver failure, and hepatotoxicity. Herbal extracts have historically been employed in the treatment of various human diseases. RES is an endogenous agent found in foodstuffs such as grape, blueberry, and peanut (26). Studies of the biological activities of RES have shown that it exhibits antioxidant, anti-inflammatory, antiapoptotic, anticancer, antiatherogenic, and cardioprotective properties (9). In their clinical study, Nguyen et al. (2009) reported the potential effects of RES on colorectal and prostate cancer in particular, and stated that the preoperative administration of RES exhibited beneficial effects in patients with colorectal cancer (27). Patel et al. (2010) showed that the administration of RES once daily for eight days prior to colon resection in 20 patients aged 46-83 reduced cell proliferation in tumor tissue (28).

Some studies in the literature have reported that treatment with RES reduces tissue damage associated with villous atrophy and shedding in the jejunum, produces an increase in villous length, and significantly improves intestinal cell morphology (29,30). Dong et al. (2013) reported preservation of the lamina propria despite partial villous damage, and significantly lower intestinal damage scores, following 50 mg/kg RES administration in the damaged intestinal wall with loss of villous structure and severe necrosis (31). Another study of severe mucosal damage ranging from villous loss with leukocyte infiltration and necrosis to mucosal infarction reported that 15 mg/kg application of RES prevented damage occurring in the crypts, but that villous loss could not be reduced with the use of RES (32). In another study, morphological changes such as a necrotic epithelium in intestinal tissue, mucosa ulceration, and widespread inflammatory cell infiltration in the mucosa and submucosa decreased after RES treatment (10 mg/kg) and that the mucosal architecture was preserved (33). In agreement with the previous literature, the results of the present study show that apical surface epithelial degeneration, villar fusion, and inflammatory cell infiltration decreased significantly in the CP+RES30, CP+RES60, and CP+RES90 groups compared to the CP group. Shedding and degeneration of epithelial cells and their microvilli also decreased, while villous structures were preserved. Although the histological findings of the treatment groups were similar to one another, damage score values decreased significantly, especially in the CP+RES30 group, compared to the CP group.

Studies have reported that due to the natural high sensitivity of the rapidly proliferating intestinal epithelium, the use of the chemotherapeutic agent CP and other radiotherapeutic approaches renders the metabolically active intestinal mucosa highly susceptible to cytotoxic effects and may cause an increase in intestinal apoptosis (34). Bodiga et al. (2012) developed an acute intestinal injury model in rats through the intraperitoneal injection of the broad spectrum antitumor drug CP at a dose of 2.61 mg bodyweight. Those authors determined that CP caused apoptosis in the villus and crypt and that the rapidly proliferating crypt region was more sensitive to CP, with higher rates of apoptosis (35). In their study of CP-induced intestinal injury, Hu et al. (2021) showed that exposure to 20 mg/kg CP caused an increased in the numbers of TUNEL-positive intestinal cells (17). Another study reported significantly fewer apoptotic cells in mice treated with RES (29). AI findings evaluated using the TUNEL method in the present study were significantly higher in the CP group. AI values in the treatment groups decreased significantly compared to the CP group. While no significant difference in AI values was observed between the CP+RES30 and CP+RES60 groups, these were significantly higher in the CP+RES90 group than in the CP+RES30 group. These results suggest that dosages of 30 and 60 mg/kg RES may be sufficient in terms of antiapoptotic efficacy, while a dosage of 90 mg/kg may be excessive and capable of reducing the antiapoptotic effects of RES.

Tumor necrosis factor-alpha (TNF-α) is a proinflammatory cytokine (signaling molecule) produced by the immune system. It plays an important role in inflammation and apoptosis signaling. TNF-α is also an important step in the initiation of an inflammatory response (36). Interleukin-1 beta (IL-1β), another proinflammatory cytokine, is a protein molecule released in conditions such as inflammation and tissue damage (37). In the present study, TNF-α values in the CP group were significantly higher than those in the control group. However, TNF-α values in the treatment groups were significantly lower compared to those in the CP group. No significant difference was observed between the CP+RES30 and CP+RES60 treatment groups, but TNF-α levels in the CP+RES90 group were significantly higher than those in the CP+RES30 group. Some studies investigating CP-induced intestinal damage have reported findings consistent with our own results, with exposure to CP significantly increasing TNF-α levels in mice (17,38). The anti-inflammatory effect of RES derives from its ability to inhibit the synthesis and release of inflammatory mediators (39). Parlar and Arslan (2019) examined the effects of RES on TNF-α following ischemic injury and reported that RES administration at 15 mg/kg once daily for five days prior to surgery significantly lowered increased TNF-α activity (40). Another study reported that RES reduced TNF-α values that had risen as a result of intestinal injury (30). These studies support our findings regarding the anti-inflammatory effects of RES. However, no significant variation was found between the experimental groups in terms of score findings for IL-1β that we used to determine proinflammatory cytokine levels. In their investigation of intestinal injury resulting from CP, Hu et al. (2021) reported, in contrast to the present study, that exposure to CP significantly increased IL-1β levels in mice (17). Nardini et al. similarly detected mucosal damage, inflammation, and rising IL-1β levels in mice receiving CP treatment (41). Another study of the protective and anti-inflammatory effects of RES also found that RES significantly reduced increased IL-1β activity (40).

Study Limitations

Our research findings should be supported by different parameters and analysis methods. Different studies are needed for dose evaluation.

Conclusion

In conclusion, CP was observed to render the metabolically active intestinal mucosa highly susceptible to cytotoxic effects, resulting in severe histological tissue damage, intestinal apoptosis, and an increase in proinflammatory cytokines. The administration of RES, a potent antioxidant, prior to CP treatment in rats was found to exhibit a protective effect against CP-induced intestinal damage, apoptotic cell death, and proinflammatory cytokines, particularly at dosages of 30 and 60 mg/kg. We also think that our results will serve as a useful reference in determining suitable dose intervals for future RES studies.

Acknowledgements: *None*

Ethical Approval: *Permission was obtained from Harran University animal experiments local ethical committee (HAYDEK) (study protocol license no. 2022/006/20).*

Author Contributions: *Concept: HH, ST Literature Review: HH Design: HH, ST Data acquisition: HH, ST Analysis and interpretation: HH, ST Writing manuscript: HH Critical revision of manuscript: HH*

Conflict of Interest: *The author(s) do not have any potential conflict of interest regarding the research, authorship and/or publication of this article.*

Financial Disclosure: *This research received no specific grant from any funding agency in the public, commercial, or not-for-profit sectors.*

References

1. Dugbartey GJ, Peppone LJ, de Graaf IA. An integrative view of cisplatin induced renal and cardiac toxicities: molecular mechanisms, current treatment challenges and potential protective measures. Toxicology. 2016; 371:58-66.
2. Pabla N, Dong Z. Cisplatin nephrotoxicity: mechanisms and renoprotective strategies. Kidney Int. 2008; 73(9):994-1007.
3. Florea AN, Busselberg D. Cisplatin as an anti-tumor drug: cellular mechanisms of activity, drug resistance and induced side effects. Cancers. 2011; 3(1):1351-71.
4. Hassan I, Chibber S, Naseem I. Vitamin B2: a promising adjuvant in cisplatin based chemoradiotherapy by cellular redox management. Food Chem Toxicol. 2013; 59:715-23.
5. Figueiras TS, Neves-Petersen MT, Petersen SB. Activation energy of light induced isomerization of resveratrol. J Fluoresc. 2011; 21(5):1897-906.
6. Xin X, Dang H, Zhao X, et al. Effects of Hypobaric Hypoxia on Rat Retina and Protective Response of Resveratrol to the Stress. Int J Med Sci. 2017; 17:14(10):943-50.
7. Hurst WJ, Glinksi JA, Miller KB, et al. Survey of the trans-resveratrol and trans-piceid content of cocoa-containing and chocolate products. J Agric Food Chem. 2008; 56(18):8374-8.
8. Xiao Q, Zhu W, Feng W, et al. A review of resveratrol as a potent chemoprotective and synergistic agent in cancer chemotherapy. Front Pharmacol. 2019; 9:1534.
9. Xin X, Dang H, Zhao X, et al. Effects of Hypobaric Hypoxia on Rat Retina and Protective Response of Resveratrol to the Stress. Int J Med Sci. 2017; 14(10):943-50.
10. Fındık H, Tumkaya L, Yılmaz A, et al. The protective effects of astaxanthin against cisplatin-induced retinal toxicity. Cutan Ocul Toxicol. 2019; 38(1):59-65.
11. Yulug E, Turedi S, Alver A, et al. Effects of resveratrol on methotrexate-induced intestinal injury. Bratisl Lek Listy. 2015; 116(11):676-80.
12. Potten CS. What is an apoptotic index measuring? A commentary. Br J Cancer. 1996; 74:1743-8.
13. Kaymaz A, Ulas F, Erimsah S, et al. Investigation of the effect of quercetin in an experimental oxygen-induced retinopathy model. Exp Biomed Res. 2021; 4(2):131-40.
14. Rottenberg S, Disler C, Perego P. The rediscovery of platinum-based cancer therapy. Nat Rev Cancer. 2021; 21(1):37-50.
15. Farooqui Z, Ahmed F, Rizwan S, et al. Protective effect of Nigella sativa oil on cisplatin induced nephrotoxicity and oxidative damage in rat kidney. Biomed Pharmacother. 2017; 85:7-15.
16. Ghosh S. Cisplatin: The first metal based anticancer drug, Bioorg Chem. 2019; 88:102925.
17. Hu JN, Yang JY, Jiang S, et al. Panax quinquefolium saponins protect against cisplatin evoked intestinal injury via ROS-mediated multiple mechanisms. Phytomedicine. 2021; 82:153446.
18. Shahid F, Farooqui Z, Khan F. Cisplatin-induced gastrointestinal toxicity: an update on possible mechanisms and on available gastroprotective strategies. Eur J Pharmacol. 2018; 827:49-57.
19. Conklin KA. Dietary antioxidants during cancer chemotherapy: impact on chemotherapeutic effectiveness and development of side effects. Nutr Cancer. 2000; 37(1):1-18.
20. Chang B, Nishikawa M, Sato E, et al. L-Carnitine inhibits cisplatin induced injury of the kidney and small intestine. Arch Biochem Biophys. 2002; 405(1):55-64.
21. Shahid F, Farooqui Z, Rizwan S, et al. Oral administration of Nigella sativa oil ameliorates the effect of cisplatin on brush border membrane enzymes, carbohydrate metabolism and antioxidant system in rat intestine. ExpToxicolPathol. 2017; 69(2):299-306.
22. Zou YT, Zhou J, Wu CY, et al. Protective effects of Poria cocos and its components against cisplatin-induced intestinal injury. Ethnopharmacol. 2021; 269:113722.
23. Zhang JJ, Wang S, Gao XF, et al. Arabinogalactan derived from Larix gmelinii (Rupr.) Kuzen. Alleviates cisplatin-induced acute intestinal injury in vitro and in vivo through IRE1α/JNK axis mediated apoptotic signaling pathways. Int J Biol Macromol. 2022; 209(Pt A):871-884.
24. Jin S, Zhu T, Deng S, et al. Dioscin ameliorates cisplatin-induced intestinal toxicity by mitigating oxidative stress and inflammation. Int Immunopharmacol. 2022; 111:109111.
25. Yilmaz Y, Tumkaya L, Mercantepe T, et al. Protective effect of astaxanthin against cisplatin-induced gastrointestinal toxicity in rats. Eur Surg. 2022; 54:32-8.
26. Valentovic MA. Evaluation of Resveratrol in Cancer Patients and Experimental Models. Adv Cancer Res. 2018; 137:171-88.
27. Nguyen AV, Martinez M, Stamosm MJ, et al. Results of a phase I pilot clinical trial examining the effect of plant-derived resveratrol and grape powder on Wnt pathway target gene expression in colonic mucosa and colon cancer. Cancer Manag Res. 2009; 1:25-37.
28. Patel KR, Brown VA, Jones D, et al. Clinical pharmacology of resveratrol and its metabolites in colorectal cancer patients. Cancer Res. 2010; 70(19):7392-9.
29. Zhang H, Yan H, Zhou X, et al. The protective effects of Resveratrol against radiation-induced intestinal injury. BMC Complement Altern Med. 2017; 17(1):410.

30. Cheng K, Song Z, Li S, et al. Effects of resveratrol on intestinal oxidative status and inflammation in heat-stressed rats. J Therm Biol. 2019; 85:102415.
31. Dong WP, Li FF, Pan ZG, et al. Resveratrol ameliorates subacute intestinal ischemia-reperfusion injury. J Surg Res. 2013; 185(1):182-9.
32. Yildiz F, Terzi A, Coban S, et al. Protective effects of resveratrol on small intestines against intestinal ischemia-reperfusion injury in rats. J Gastroenterol Hepatol. 2009; 24(11):1781-5.
33. Martín AR, Villegas I, La Casa C, et al. Resveratrol, a polyphenol found in grapes, suppresses oxidative damage and stimulates apoptosis during early colonic inflammation in rats. Biochem Pharmacol. 2004; 67(7):1399-410.
34. Pandit A, Kim HJ, Oh GS, et al. Dunnione ameliorates cisplatin-induced small intestinal damage by modulating NAD(+) metabolism. Biochem Biophys Res Commun. 2015; 467(4):697-703.
35. Bodiga VL, Bodiga, Surampudi S, et al. Effect of vitamin supplementation on cisplatin-induced intestinal epithelial cell apoptosis in Wistar/NIN rats. Nutrition. 2012; 28(5):572-80.
36. Brennan FM, Maini RN. Role of pro-inflammatory cytokines in rheumatoid arthritis. Springer Seminars in immunopathol. 1998; 20(1-2):133-47.
37. 37. Jain S, Gautam V, Naseem S. Acute-phase proteins: As diagnostic tool. J Pharm Bioallied Sci. 2011; 3(1):118-27.
38. Aydin I, Kalkan Y, Ozer E, et al. The protective effect of infliximab on cisplatin-induced intestinal tissue toxicity. Eur Rev Med Pharmacol Sci. 2014; 18(14):2076-83.
39. Velmurugan BK, Rathinasamy B, Lohanathan BP, et al. Neuroprotective role of phytochemicals. Molecules. 2018; 23(10):2485.
40. Parlar A, Arslan S. Resveratrol Normalizes the Deterioration of Smooth Muscle Contractility after Intestinal Ischemia and Reperfusion in Rats Associated With an Antioxidative Effect and Modulating Tumor Necrosis Factor Alpha Activity. Ann Vasc Surg. 2019; 61:416-426.
41. Nardini P, Pini A, Bessard A, et al. GLP-2 Prevents Neuronal and Glial Changes in the Distal Colon of Mice Chronically Treated with Cisplatin. Int J Mol Sci. 2020; 21(22):8875.